行政院國家科學委員會專題研究計畫　期中進度報告

捷運地下車站火災煙流分析與人流測試(1/2)

計畫類別：個別型計畫

計畫編號：NSC91-2212-E-002-089-

執行期間：91 年 08 月 01 日至 92 年 09 月 30 日

執行單位：國立臺灣大學應用力學研究所

計畫主持人：陳發林

報告類型：精簡報告

處理方式：本計畫可公開查詢

中　華　民　國 92 年 5 月 13 日

行政院國家科學委員會專題研究計劃成果報告
捷運地下車站人流分佈與通風策略研究（1/2）

計劃編號:NSC 91-2122-E-002-089
執行時間:91/08/01 ~ 92/07/31

主持人: 陳發林教授 研究生：張文嘉、溫英志先生
執行單位：國立台灣大學 應用力學所

Abstract

In fires of subway stations, the most immediate threat to passenger's life is not the direct exposure to fire, but the smoke inhalation because it contains hot air and toxic gases. To understand the mechanisms driving the motion of smoke is therefore an important issue of fire safety, and the stack effect is found to be an important mechanism having significant influence. In this paper, we compute the three-dimensional smoke flow fields under various fires happened in a representative subway station of Taipei Rapid Transit System. To clarify the mechanisms corresponding to the stack effect, a simplified three-dimensional configuration is also considered. Results indicate that, without mechanical smoke control, the stack effect plays a decisive role and is virtually the sole factor influencing the smoke movement. Because of the stack effect, most or sometimes all of the smoke will choose a vertical shaft (usually a stairwell) to evacuate, and the cross sectional area of the shaft and the location of fire determine which shaft is chosen. Present computational results show the evidences of the importance of the stack effect and provide both valuable information to the design of the passenger evacuation routes in fires as well as criteria to the design of smoke control systems of subway stations.

1. Introduction

In building fires the air becomes hot and less dense due to combustion. A strong buoyancy force is induced, leading the air containing smoke to move upwards along the vertical shaft of building. Then a stream moving to the shaft is forming, sucking the surrounding air and smoke towards the direction of the shaft. This phenomenon is known as stack effect (or chimney effect), one of the major driving forces of the smoke movement in building fires. In most situations of building fires, the pressure difference induced by the stack effect is much larger than that due to other driving forces, such as the expansion of combustion gas, the wind effect, and so on [1]. As soon as the stack effect forms, the smoke generated in the building will move towards and into vertical shafts, such as stairwells, the shafts of elevators, and the vertical shafts of the ventilation system, becoming an important phenomenon which the designer of the smoke control system has to consider seriously. The stack effect is also crucial in the design of the heating and cooling system of buildings, especially in the calculation of the infiltration rate in a building envelope through the combination with the wind effect [2]. The details of the physical mechanisms relevant to the stack effect are reviewed by Zukoski [3], in which the model development for the computation of relevant flows is emphasized.

The stack effect also plays a significant role in the smoke control of subway stations because there are various structural vertical spaces in the station through which the buoyancy force of hot smoke will be enhanced. A good example is the Gong-Guan Subway Station (GGSS), a typical mid-way station in the Taipei Rapid Transit System (TRTS). The TRTS consists of six lines and 63 stations, totally 86.8km long, serving to commute about a million passengers per day, and will be virtually doubled in size within next few years. As a typical subway station the GGSS has two floors (Fig. 1), one is the platform floor on the bottom and the other is the lobby floor on the top. On the two ends of the lobby floor, there are hallways connecting the lobby and the stairwell. The length of the station is 142.1m and the width is 17.9m. The height of the lobby floor is 4.15m and that of the platform floor is 5.15m. To enhance the beauty of the interior of the station and to relax the mental pressure imposed by the space limitation in the platform floor, a large area of the lobby floor at center is cut off (Fig. 1), remaining two two-meter-width passages on the two sides of the lobby floor and two hallways at the two ends connecting the side-passages and the stairwells. This cut-off of the central portion of the lobby floor, unfortunately, enhances the buoyancy force of hot smoke, making the smoke control in the GGSS more difficult.

In such a subway station, the stack effect plays a crucial role in smoke control because there are four vertical shafts (or exits) located on the four corners of the station. The four exits in the GGSS direct respectively to the campus of National Taiwan University (NTU), the Shuei-Yuan traditional market and the South-East Asia Theater. All these places are busy-life areas, so that the GGSS serves to commute more than 20,000 passengers per day. Each exit is accompanied with a stairwell connecting the lobby floor and the surface road, forming a vertical space through which the stack effect may be enhanced to predominate the smoke movement in station fires. The present paper is aimed to illustrate the predominance of the stack effect in the GGSS, which may account for a representative example to other subway stations of similar architectural design. As smoke moves into stairwells, the evacuation of people from subway station through these exits is prohibited, influencing dramatically the whole evacuation plan in fire emergency.

Fires in subway stations happened frequently in history, especially in the past two decades when subways become a major transportation scheme in metropolitan areas. Three well-known accidents causing a large amount of victims happened in London King's Cross subway station, Baku (the capital of Republic of Azerbaijan) subway tunnel, and Daegu of South Korea. The fire in King's Cross happened on November 18, 1987, causing 87 people either to die or suffering from serious injuries. The fire in Baku happened in October 29, 1995, which was even more serious, the hot air and toxic smoke killed 337 people and left 227 seriously injured. The fire in Daegu happened very recently on February 18, 2003. Two trains carrying about 1000 passengers were burned by explosive fires set by a man having mental health problems. In less than 1 hour, more than 200 people died and about 400 injured. People were burned, trampled and suffocated to death in the smoke-filled subway station and the trains. The results obtained from the computational fluid dynamics (CFD) simulation of the King's Cross fire [4] imply that the stack effect predominates the smoke movement in this complicated-structured station, resulting in that buoyant smoke moves rapidly through the stairwells and blocks the ways people supposed to evacuate.

In the present paper, we employ CFD to investigate the smoke flow in the GGSS, special emphasis is placed on the stack effect. The mathematical model comprising the conservation laws of momentum, heat and mass of the smoke flow is considered, in which the turbulent mixing governed by the $\kappa-\varepsilon$ model is included. A computer code, named CFX4, developed by AEA Co. of England is employed to solve the flow field. In this code the finite volume numerical scheme is employed. In the following, we present the mathematical model in section 2, but the details of the numerical approach are referred to the manual of CFX4 code. We study the characteristics of the stack effect in section 3 by considering a specially designed but simplified configuration. The stack effect in the GGSS is shown in section 4, several examples clearly illustrate its prominence. Finally, concluding remarks are drawn in section 5.

With these CFD results, one may gain ideas for the design of smoke control in subway stations.

2. Mathematical model

To study the smoke propagation in GGSS, we employ the CFD approach to investigate the flow field in the three-dimensional configuration of the subway station. Reliable CFD results regarding the smoke movement in fires can be obtained only when the following points are carefully treated [5]: (1) The flow in the subway station, especially that near the fire, shall be three-dimensional. (2) A careful choice of a turbulence model and the corresponding input parameters is crucial; it was found that the $k-\varepsilon$ turbulence model can well simulate the flow in the fire. (3) The fire can be taken as a source of heat and smoke (accounted for by CO_2 [6]) in which no combustion is considered. The parameters used and the model chosen in the present study are the same as those used in tunnel fire computations [5], to which the reader is referred.

The following Reynold's averaged equations serve well to simulate this 3D turbulent flow in which a source of heat and smoke are present [7]. They are

the continuity equation

$$\frac{\partial \rho}{\partial t} + \nabla \bullet (\rho \underline{U}) = 0 , \tag{1}$$

the momentum equations

$$\frac{\partial}{\partial t}(\rho \underline{U}) + \nabla \bullet (\rho \underline{U}\,\underline{U}) = \rho \underline{g} + \nabla \bullet \underline{\underline{\sigma}} , \tag{2}$$

the energy equation

$$\frac{\partial}{\partial t}(\rho H) + \nabla \bullet (\rho \underline{U} H) = \nabla \bullet (\lambda \nabla T) + \nabla \bullet \left(\frac{\mu_t}{\sigma_H} \nabla H \right) + \frac{\partial p}{\partial t} + \rho \underline{g} \bullet \underline{U} + \nabla \bullet \left(\mu_e (\nabla \underline{U} + \nabla \underline{U}^T - \frac{2}{3} \nabla \bullet \underline{U}\,\underline{I}) \underline{U} \right) + Q \tag{3}$$

the transport equation for Y_c, the mass fraction of CO_2

$$\frac{\partial}{\partial t}(\rho Y_C) + \nabla \bullet (\rho \underline{U} Y_C) = \nabla \bullet ((\kappa + \frac{\mu_t}{\sigma_c})\nabla Y_C) + S_C \tag{4}$$

the transport equation for the turbulent kinetic energy k

$$\frac{\partial}{\partial t}(\rho k) + \nabla \bullet (\rho \underline{U} k) = \nabla \bullet ((\mu + \frac{\mu_t}{\sigma_k})\nabla k) + P + G - \rho\varepsilon \tag{5}$$

the transport equation for the turbulent dissipation rate ε

$$\frac{\partial}{\partial t}(\rho\varepsilon) + \nabla \bullet (\rho \underline{U} \varepsilon) = \nabla \bullet ((\mu + \frac{\mu_t}{\sigma_\varepsilon})\nabla \varepsilon) + C_1 \frac{\varepsilon}{k}(P + C_3\, max(G,0)) - C_2 \rho \frac{\varepsilon^2}{k}$$

equation of state

$p = \rho RT$,

and the constitutive equation, $h = h(T, p)$, assumed to have the following analytic form,

$$h = C_p(T - T_0). \tag{8}$$

In above equations, ρ accounts for the density, $\underline{U}$ the velocity vector (u, v, w), $\underline{g}$ the acceleration due to gravity, λ the heat conductivity, T the temperature, p the pressure, Q the heat source which is specified in the region of the fire, κ the diffusivity of CO_2 in air, S_C the mass source of CO_2 which is also specified only in the region of the fire, the stress is

$$\underline{\underline{\sigma}} = -p\underline{I} - \frac{2}{3}\rho k \underline{I} + \mu_e(\nabla \underline{U} + \nabla \underline{U}^T) - (2/3)\mu_e(\nabla \bullet \underline{U})\underline{I} \tag{9}$$

the mean total energy is

$$H = h + \frac{\underline{U} \bullet \underline{U}}{2} + k \tag{10}$$

the shear production is

$$P = \mu_e \nabla \underline{U} \bullet \left(\nabla \underline{U} + (\nabla \underline{U})^T\right) - \frac{2}{3}\nabla \bullet \underline{U}\left(\mu_e \nabla \bullet \underline{U} + \rho k\right) \tag{11}$$

and the shear production due to buoyancy is

$$G = -\frac{\mu_t}{\rho\sigma_\rho} \underline{g} \bullet \nabla\rho$$

In addition, T_0 is a reference temperature where h is defined to be zero. Note that the use of the $k-\varepsilon$ model yields $\mu_e = \mu_t + \mu$ where $\mu_t = \rho C k^2 / \varepsilon$, $C = 0.09$, and μ is the dynamic molecular viscosity [7]. The values of the Prandtl numbers, σ_h, σ_k, σ_ε, and σ_ρ, and the values of the three coefficients C_1, C_2, and C_3 are listed in Table 1, which are the same as those of [5]. Equations (1) to (8) are the governing equations of the unsteady, turbulent, three-dimensional, compressible flow. Based on these equations, the geometry of the interior space of GGSS, and the initial and boundary conditions of the flow field, the distributions of the unknown quantities ρ, $\underline{U}$, p, h, T, Y_c, k, and ε, in the flow field will be determined.

To solve the above equations, we employ the CFX4 code. The computational domain will be either a three-dimensional simple configuration (section 3) to study the characteristics of the stack effect or the three-dimensional GGSS (section 4, Fig. 2) to realistically study the stack effect of the smoke movement in the subway stations. Note that in the present paper we do not consider combustion; so the fire is considered as the source of heat and smoke. As found from the product analysis of combustion, a fire having a heat release rate of 5MW is accompanied with a smoke generation rate of $1.4 \times 10^5\ ppm/s$ [8], both are fixed in present paper. Nevertheless, for convenience in the following discussions, "fire" will be used to mean a heat-smoke source.

In the present paper, two computational fields are considered and both are three-dimensional. The first is a simple enclosure as shown on the top of Figs. 3 to 8 and the second is the GGSS as shown in Figs. 1 and 2. Both configurations are embedded with a multi-grid system, in which the space is divided into numerous blocks. In each block the grid is uniformly distributed, but the grid sizes of the blocks can be different from each other, depending on the characteristics of the flow. For example, the grid size in the block containing the fire or being near to is three times finer than that away from the fire; the grid near corners where the flow changes rapidly is two times finer than that without geometry change. The number of cells for the enclosure is about 21 thousand and that for the GGSS is more than 245 thousand.

Regarding the boundary conditions, we note that the flow in GGSS is primarily enclosed by rigid walls with some openings of relatively small area. On the rigid walls the conditions are specified as no slip, no penetration (zero flux), and adiabatic for momentum, CO_2, and the temperature, respectively. Since the $k-\varepsilon$ model is sensitive near the walls, the well-known wall function is employed so that the direct integrations of the equations of k and ε through this region can be avoided. At all openings to the atmosphere, the atmospheric pressure instead of the detailed velocity distributions is given. In the portions of the openings where the fresh air flows in, the mass fraction of CO_2, and the temperature of surrounding atmosphere are specified. However, it is difficult to specify the turbulence quantities across these portions. A common remedy is to set the values for k and ε based on local mean flow characteristics. In the other portions where hot air and "smoke" flows out, the fully developed flow approximation is assumed for the transported species (CO_2), velocity, k, ε, and temperature.

3. Characteristics of the stack effect

To study the characteristics of the stack effect, we construct a simplified configuration consisting of a rectangular space of size 100x10x10 m^3 and two elbow-shaped vertical shafts of different cross sectional areas. A fire is imposed in the interior of the rectangular space and the movement of the smoke is examined to help understand the characteristics of the stack effect. Regarding boundary conditions, we imposed constant temperature, zero smoke concentration and no-slip condition at the wall and use constant pressure and constant heat and mass fluxes on the exit plane of the shaft. At the beginning of the computation, the air in the enclosure is motionless and the temperature is uniformly 298^{o}K (room temperature 25^{o}C) and no heat or mass source are released. To check the correctness of the computational results, we examine the conservation of mass in the enclosure by calculating the mass flow passing the two shafts. These mass-flow rates shall balance with the mass source generated from the fire. This check is done in each time step, and is found to be satisfactory always.

In Figs. 3 to 11 we illustrate the temperature distributions in both the enclosure and the GGSS by colors. Roughly speaking, for example, dark blue accounts for 298^{o}K and below, green for 348^{o}K, yellow for 398^{o}K, light orange for 448^{o}K, orange for 498^{o}K or higher. The continuous change of the temperature is accounted for by a continuous spectrum of color. We have no intention to employ the CFD approach to claim the accuracy of the present results in a quantitative sense. We rather look for a qualitative trend of the smoke-flow in fires. With this qualitative view in mind, we believe that the characteristics of the smoke flow, and especially the stack effect in the simplified enclosure and the subway station, can be well described.

In Fig. 3 the fire is located in the middle of the enclosure and the cross sectional areas of the two shafts are respectively 2x5 m^2 and 6x5 m^2. At the beginning the smoke rises from the fire on the bottom, impinges onto the ceiling and separates into two streams of equal mass-flow rate and propagates, respectively, towards the right and left shafts (Fig. 3(a)). The two streams reach the shafts at almost the same time (Fig. 3(b)). Then the smoke in the left shaft (of smaller cross sectional area) rises along the vertical channel with higher speed than that in the right shaft, inducing a lower pressure in the left shaft than in the right shaft. A horizontal pressure gradient is thus formed and, eventually, all of the smoke in the rectangular space is driven to move towards the left shaft. As indicated by Zukoski (1995), two major mechanisms are responsible for the flow induced by the stack effect: Firstly, the pressure difference between the air in the shaft and the surroundings (i.e. the horizontal pressure gradient); secondly, the turbulent mixing between the hot and cold air. In the present case, obviously, the first mechanism dominates in the early stage of the flow formation, and the second mechanism is gradually playing a more important role as the stack effect becomes more rigorous.

As we reduce the area-difference between the two shafts from $4\times 5m^2$ to $2\times 5m^2$ (Fig. 4), the stack effect is enhanced since the generated smoke is sucked out of the rectangular space through the shaft of smaller area within a shorter time. This is because a larger area of the smaller shaft allows a larger mass-flow rate of smoke, making the smoke be evacuated faster. This scenario is confirmed again by the case of Fig. 5, in which the area-difference is also $2\times 5m^2$ while the areas of both exits increase, and the time to evacuate the smoke is reduced further.

We have seen from the previous cases the smoke prefers the shaft of smaller area when the fire sits in the middle between two shafts. This is the so-called area factor of the stack effect. This scenario, however, is no longer valid when the fire is not located in the middle, as shown by the examples of Figs. 6 to 8. This shall be called the location factor, which generally is predominant over the area factor as far as the stack effect is concerned. In Figs. 6 to 8 we use the same configurations as in Figs. 3 to 5 and impose the fire $1.5m$ away from the middle but closer to the shaft of larger area. Inevitably and without exception, the smoke is evacuated from the shaft closer to the fire and of larger area. This is obviously due to the fact that the smoke reaches the closer shaft first, forming a horizontal pressure gradient to drive the smoke. From these results, a simple conclusion regarding the characteristics of the stack effect can be drawn: The shaft which the smoke reaches first will predominate over other shafts in the stack effect; namely, all the smoke in the enclosure will move to the shaft which it first reaches.

4. Stack effects in Gong-Guan subway station

The stack effect can also be significant in a more complicated configuration, such as the GGSS of Fig. 1. To compute the smoke flow in GGSS, the following boundary conditions are prescribed. On the vertical planes of the four stairwells (or exists) and of the four tunnel entrances, constant pressure as well as constant heat and mass flux conditions are prescribed. On the solid walls of the station, the no-slip condition, constant temperature and zero smoke-concentration are assumed. No mechanical ventilation system is turned on for the sake of studying the stack effect which is a natural convection phenomenon. Although the configuration of GGSS is more complicated than the case shown in Figs. 3 to 8, the characteristics of the stack effect remain.

To show this, we first impose a fire on the left of the lobby floor in GGSS, as shown in Fig. 9. At the beginning of the fire (Figs. 9a and 9b), most of the smoke moves equally to the two exits on the left hand side of the lobby floor and some of the smoke moves to the right hand side (Figs. 9c and 9d). But after the smoke starts to evacuate out of GGSS from the two exits on the left hand side, the smoke moving to the right is sucked back to the left due to the horizontal pressure gradient built by the stack effect. That is the first stage of the stack effect, showing the competition between the exits on the left- and right-hand sides of GGSS. Then, the second stage of the stack effect occurs, namely, the competition between the two exits on the left becomes significant. Since the areas of the two left-hand side exits are of small difference, the stack effect due to the area factor is not obvious (Figs. 9e and 9f) until at 4min and after (Figs. 9g to 9l). The smoke chooses Exit D to evacuate because (1) Exit D is of smaller area and (2) in front of Exit A there is a space disturbing the movement of the smoke.

In this case, the location factor dominates the smoke movement first, making the smoke move to the left-hand side of GGSS, then the area factor takes over to influence the smoke movement later, implying that Exit D serves to evacuate most of the smoke. We note that other factors due to the complex station configuration can also become influential for the smoke movement. Such factors are present in various situations and sometimes predominate over the location factor or the area factor, making the stack effect becoming more complicated and unpredictable. Nevertheless, with very few exceptions, the following rule always holds: the exit will predominate in the subway station in the evacuation of smoke when it becomes the first exit through which the smoke chooses to evacuate.

Figure 10 illustrates in a three-dimensional perspective view the smoke distribution in GGSS at 4min and 8min, respectively. At 4min, the smoke movement towards Exit D prevails, and the smoke moving to the right-hand side of GGSS starts to move back to the left. Note that the smoke moving down to the platform floor is also sucked back to the lobby floor on the left. At 8min, the stack effect becomes obvious, most of the smoke chooses Exit D to evacuate out of GGSS, and most of the space in GGSS in both lobby and platform floors are clear of smoke.

In Fig. 11 we show a case in which the fire is located in the middle of the platform floor. In such a case, the smoke moves upwards rapidly, impinges on the ceiling and then spreads over to the two ends of GGSS in the lobby floor (Figs. 11a to 11d). The smoke reaches the two ends at almost the same time, while due to the smaller-area of Exit B, the stack effect predominates the movement of smoke, inducing the smoke to move to the right (Figs. 11e to11h). However, because the quantity of smoke is so large that Exit B is not sufficiently large to evacuate all the smoke moving to the right, Exit C starts to help evacuate some of the smoke due to its large cross sectional area (Figs. 11i to 11l). This case illustrates a good example of the competition of smoke evacuation among exits of a subway station. Competition occurs in different stages, depending on the predominance of the location factor or the area factor. In the case of Fig. 11, the area factor is the sole factor influencing the smoke movement, while still having two stages of influence: Firstly, a competition between the exits on the left and right. Secondly, a competition between the two exits on the right.

5. Concluding remarks

The computational results shown in this paper indicate that there are two factors influencing the stack effect in subway stations: the area factor and the location factor. Although these two factors compete to predominate, a general rule-of-thumb is clear: the smoke will evacuate from that exit which the smoke reaches first, and then all or most of the smoke in the station will move towards this exit to evacuate. If there is no location factor, the area factor will predominate the system; i.e. the smoke will evacuate from the exit of smaller area. However, if two factors become simultaneously effective, the location factor in general is more influential than the area factor. In reality, nevertheless, the configuration of the inner space of the subway station can be more complicated than the GGSS, such as King's Cross station of London, and other factors such as the geometry may play a role. This is simply due to that various kinds of space arrangements may create disturbances on smoke movement, and in turn influence the results on the stack effect. Nevertheless, in a complicated space the rule-of-thumb of the stack effect stated is the one which people can always follow with: The smoke will evacuate out of the exit where the smoke reaches first. If the smoke reaches many exits at the same time, then the area factor will dominate.

Although we did not examine other factors as follows, which might also be influential on the stack effect in subway stations, an implication can still be made. These factors can be minor, but may become significant under certain circumstances.

(1) The initial situation of the flow in a subway station before the occurrence of a fire. This flow can be generated by the piston effect as a train moves into the station or by the wind-effect outside the station. The direction of the initial flow will surely influence the later movement of the smoke. However, since the train will either stop in stationvery soon or pass rapidly, this flow can influence the smoke movement only within a short period.

(2) The presence of the passengers and their movement. As the fire occurs, passengers are guided by alarm signals to move in a few certain directions, which may to some extent create flows and may also influence the smoke movement. Yet, this factor might not become significant after all because the smoke always moves to the upper part of the space and the passengers move in the lower part.

(3) The geometric factor in a complicated space. Smoke evacuation used to be taken as an insignificant factor to be considered in the interior design of subway stations. Consequently, for the sake of beauty or others, there may be various kinds of obstacles to block the movement of smoke, and they all may influence the smoke evacuation to various extent.

As a conclusion, the stack effect is a complicated phenomenon in subway stations. The influencing factors can vary widely although, by and large, the area and the location factors are predominating in most situations. Accordingly, the movement of smoke in a subway station can be hardly predictable. To ensure the fire safety in the subway station under an absolute standard, an active control of smoke movement shall be imposed. In the GGSS, for example, three mechanical systems serve to control smoke in fires: (1) The tunnel ventilation fans, a major mechanical equipment for smoke control as well as ventilation, (2) The under-platform exhaust system, a minor system for evacuating the polluted air near the rails, and (3) The under-ceiling smoke evacuation system, a system serving to evacuate the smoke floating below the ceiling. With these three smoke-control systems, the smoke in the GGSS due to a fire of a heat release rate smaller than 10 MW can be well controlled [9]. On the other hand, without active smoke control, the smoke may become fatal to passengers when a fire occurs.

Acknowledgements

The financial supports for this research from both SinoTech Engineering Consultant Inc. and National Science Council under grants NSC 89-2212-E-002-61 and NSC 89-2212-E-034-009 are gratefully appreciated.

References

[1] Klote JH (1989) Considerations of stack effect in building fires, NISTIR 89-4035.

[2] Tamura GT, Shaw CY (1976) Studies on exterior wall air tightness and air infiltration of tall buildings, ASHRAE Trans., 82, Part I.

[3] Zukoski EE (1995) A review of flows driven by natural convection in adiabatic shafts, Report number NIST-GCR-95-679.

[4] Simcox S, Wilkes NS, Jones IP (1988) Fire at King's Cross underground station on 18th November 1987: Numerical simulation of the buoyant flow and heat transfer, AERE-G 4677, UK.

[5] Chen F (2000), Smoke propagation in road tunnels, ASME Applied Mechanics Review, 53(8), 207-218.

[6] Malhotra HL (1995) Goods vehicle fire test in a tunnel, Proc Of the 2nd Int Conf On Safety in Road and Rail Tunnels, Granada, Spain, paper no. 28, 237-244, 3-6 April.

[7] Markatos NC, Malin MR, Cox G (1982) Mathematical modelling of buoyancy-induced smoke flow in enclosures, Int. J Heat Mass Transfer, 25, 63-75.

[8] Ingason H (1994) Heat release rate measurements in tunnel fires, Proc of the Int. Conf. On Fires in Tunnels, Boras, Sweden, 86-103, 10-11 October.

[9] Chang WJ (2001) Smoke control in fires in Gung-Guan subway station of Taipei rapid transit system, Master thesis, National Taiwan University, Taipei, Taiwan.

Table 1 The values of the parameters of the $k-\varepsilon$ turbulent model

σ_h	=1.0
σ_k	=1.0
σ_ε	=1.217
σ_ρ	=0.09
C_1	=1.44
C_2	=1.92
C_3	=0.

Figure Captions

Figure 1. A schematic drawing of the Gung-Guan Subway Station (GGSS), in which the Exit A goes to South East Asia (SEA) theater, Exit B goes to Shui-Yuan (SY) tradition market, and both Exits C and D go to the campus of National Taiwan University (NTU). Two black arrows account for the direction of train entering station. There are four stairwells of escalators connecting the platform floor and the lobby floor, two are located in the center and two on the sides.

Figure 2. The computational grid of the GGSS. There are 125 grid-blocks in the computational domain. In each grid-block, uniform grid is employed. The number of cell of each block varies, depending primarily upon the flow structure within the block. A finer grid is prescribed for the block covering a flow of more complicated structure, such as those including fire, corner, stair,.. and so on. Totally, there are more than 245 thousand grid points in the domain.

Figure 3. Stack effect due to area difference of vertical shafts. The enclosure consists of a rectangular box of size 100x10x10m^3 and two elbow-shape vertical shafts of cross sectional area 2x5m^2 and 6x5m^2. A fire of heat release rate 5MW and smoke generation rate $1.4\times10^5\ ppm/s$ is imposed on the middle of the box. Due to the stack effect, the smoke moves toward the shaft of smaller cross sectional area.

Figure 4. Another case similar to figure 2 to illustrate the stack effect. The cross sectional areas of the two vertical shafts are of smaller difference, i.e. 4x5m^2 and 6x5m^2, which implies that stack effect is enhanced; namely, the smoke evacuates from the smaller shaft in a shorter time.

Figure 5. Another case similar to figure 2 but having different cross sectional areas of the shafts: 8x5m^2 and 6x5m^2. In terms of the stack effect a similar result is seen: smoke evacuates from the smaller shaft.

Figure 6. Another case similar to figure 2 to illustrate the stack effect. The location of the fire is closer (1.5m from the middle) to the shaft with larger cross sectional area. The smoke chooses the shaft closer to the fire to evacuate.

Figure 7. A comparison case to figure 4 by enlarging the smaller shaft from 2x5m^2 to 4x5m^2: there is still no change in the direction of smoke movement, implying that the location of the fire is more significant than the area of the shaft.

Figure 8. A comparison case to figure 5 by changing the area of shaft closer to the fire from 2x5m^2 into 8x5m^2. Results show again that the smoke evacuates from the shaft closer to the fire regardless the area of shaft.

Figure 9. Smoke propagation in GGSS due to a fire located on the left of the lobby floor. All figures show the smoke distribution in the horizontal plane 1 meter below the ceiling. The stack effect can be seen from the competition between Exits A and D, and the smoke eventually chooses to evacuate from Exit D because of its smaller area.

Figure 10. Three-dimensional stereo views of the smoke propagation in GGSS, showing the cases of Figure 8 at 4min and 8min, respectively.

Figure 11. Smoke propagation in GGSS due to a fire located at the center of the bottom floor. All figures show the smoke distribution in the horizontal plane 1 meter below the ceiling. The stack effect can be seen from the competition between the exits on the left and the right and the smoke eventually evacuates from the right exits.

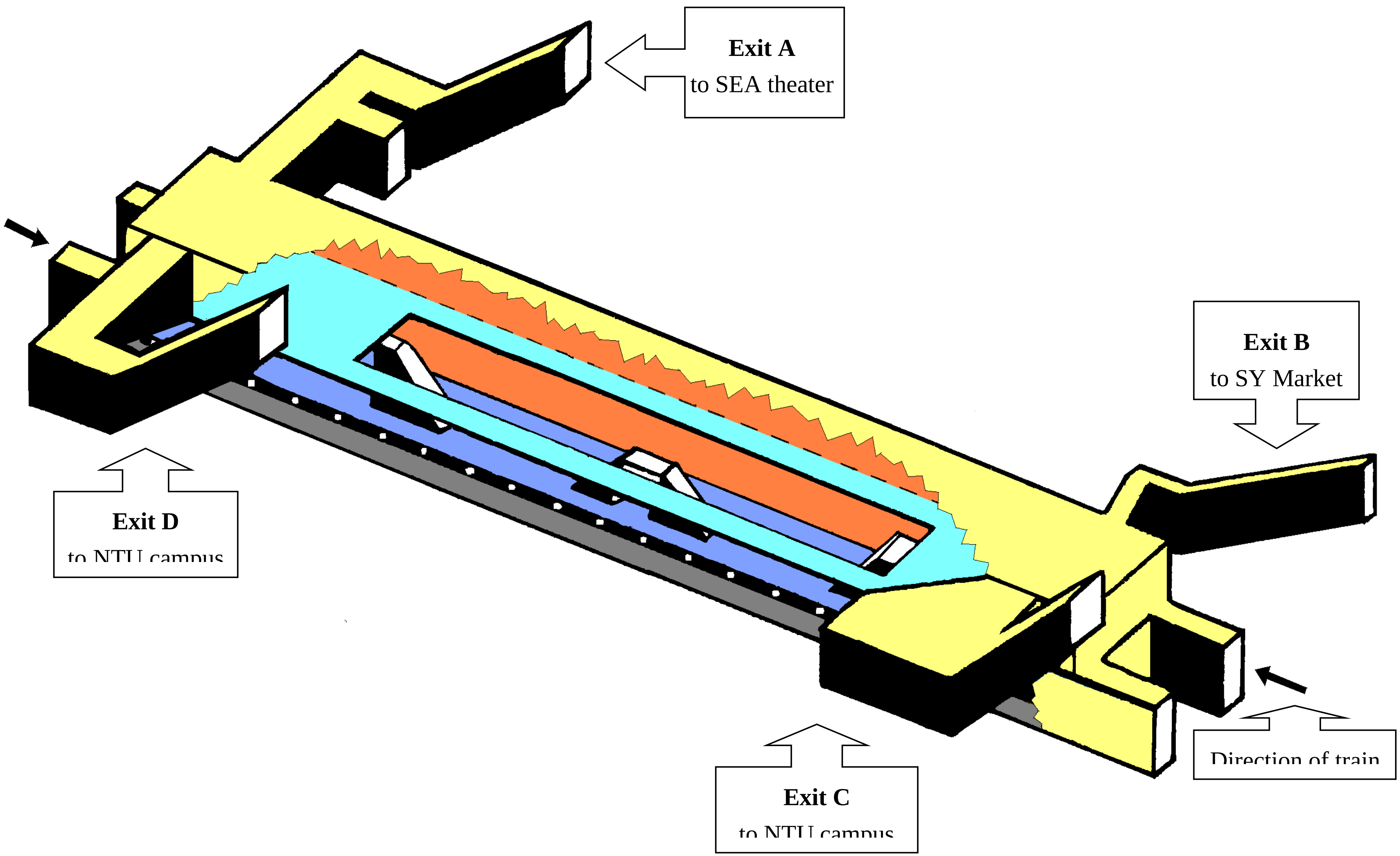

Exit A
to SEA theater
Exit B
to SY Market
Exit D
to NTU campus
Exit C
to NTU campus
Direction of train

Figure 2

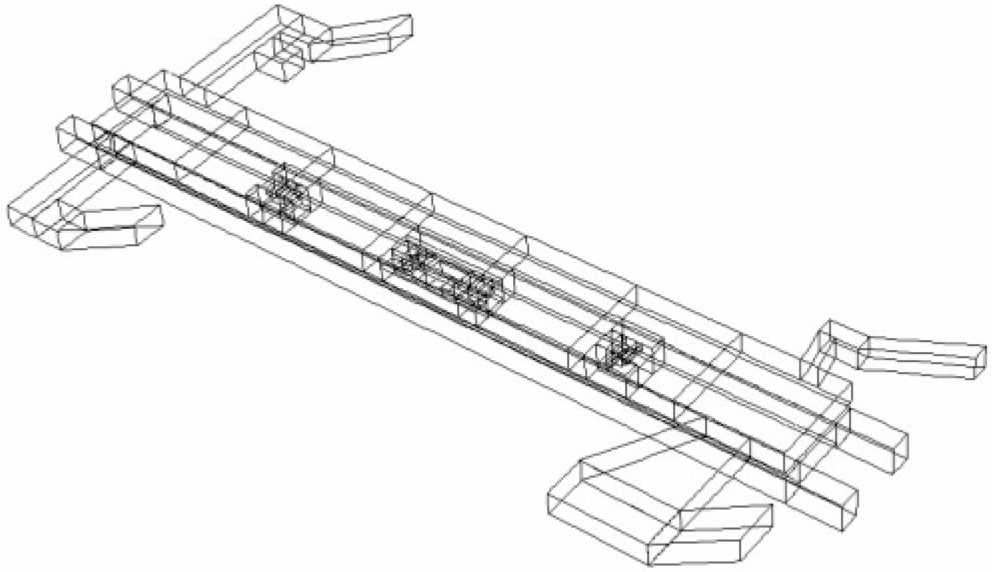

Figure 3

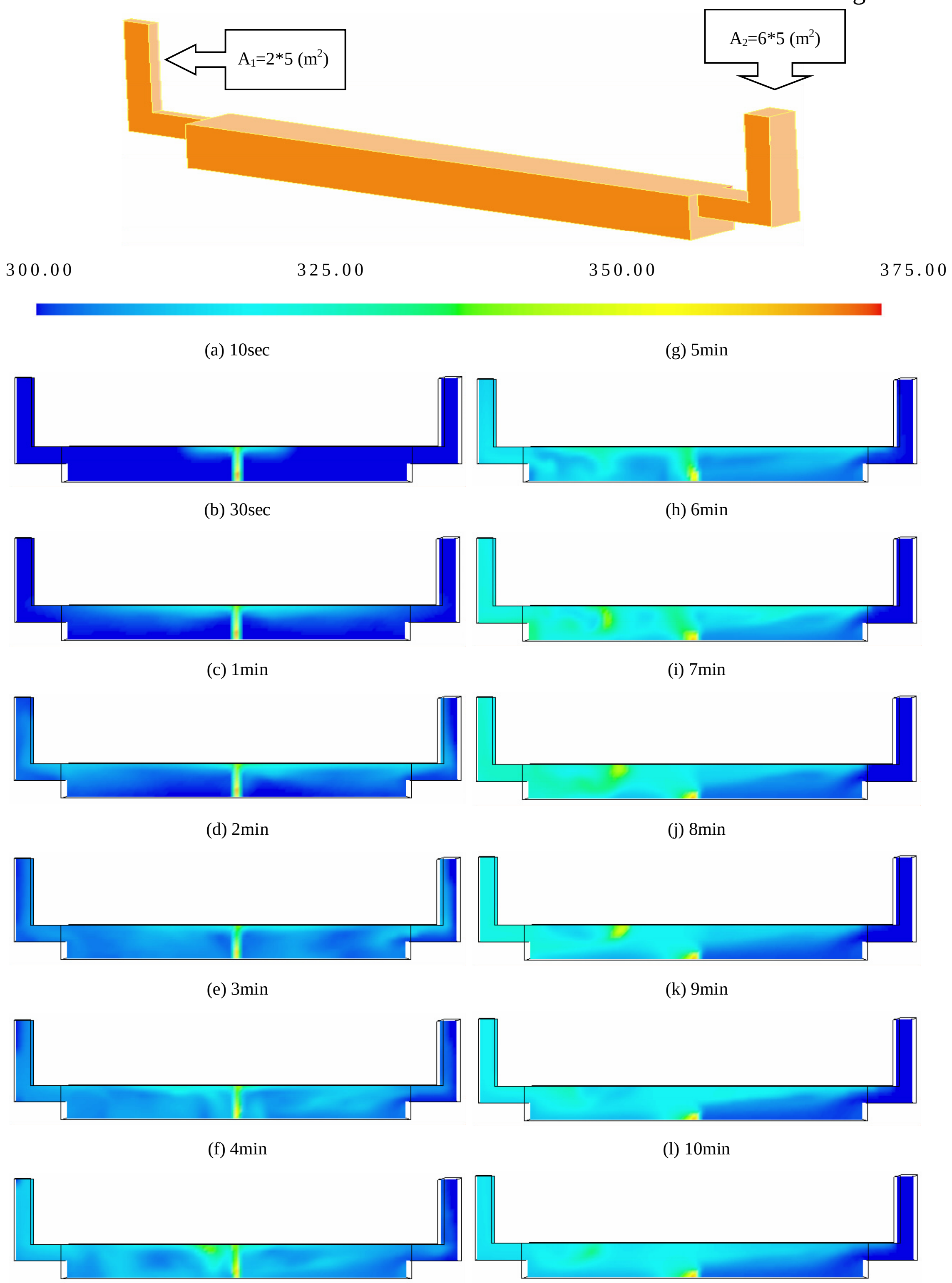

A1=2*5 (m2)
A2=6*5 (m2)
300.00
325.00
350.00
375.00
(a) 10sec
(g) 5min
(b) 30sec
(h) 6min
(c) 1min
(i) 7min
(d) 2min
(j) 8min
(e) 3min
(k) 9min
(f) 4min
(l) 10min

Figure 4

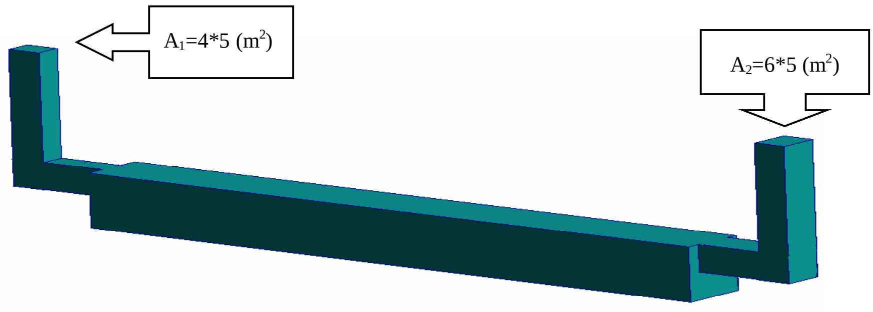

(a) 10sec

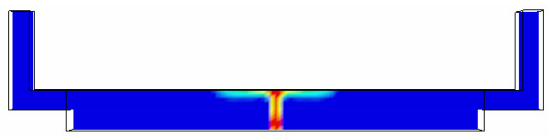

(b) 30sec

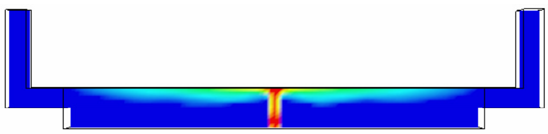

(c) 1min

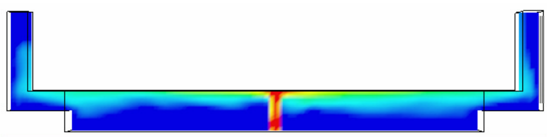

(d) 2min

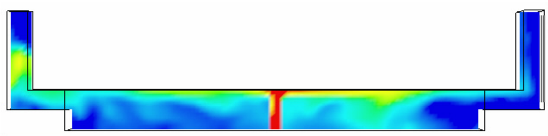

(e) 3min

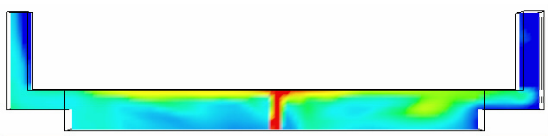

(f) 4min

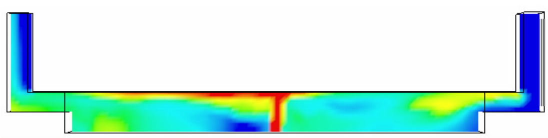

(g) 5min

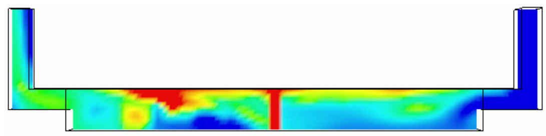

(h) 6min

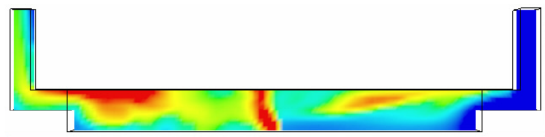

(i) 7min

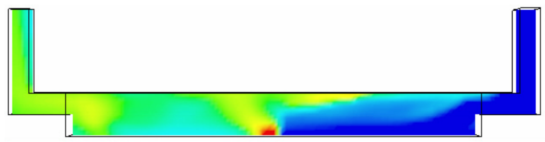

(j) 8min

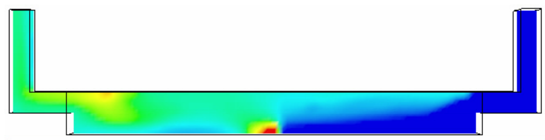

(k) 9min

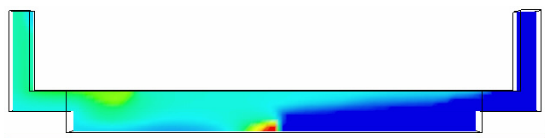

(l) 10min

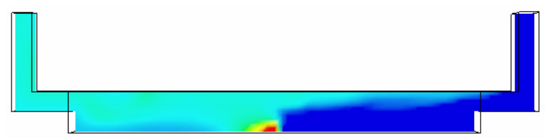

Figure 5

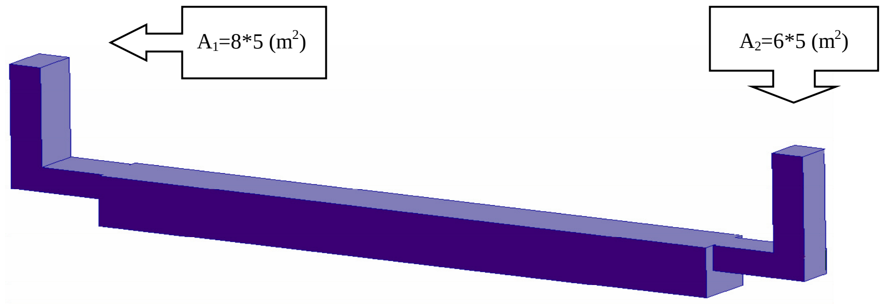

(a) 10sec

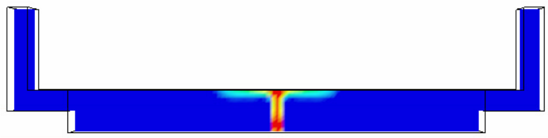

(b) 30sec

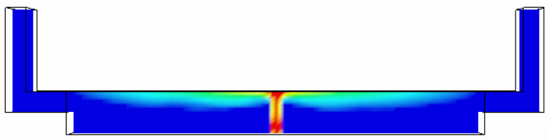

(c) 1min

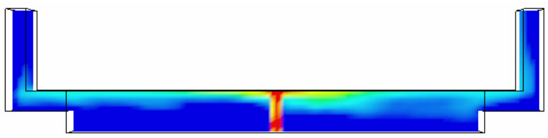

(d) 2min

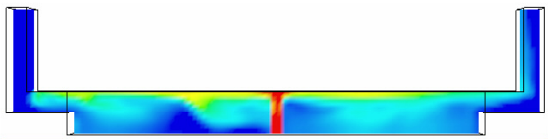

(e) 3min

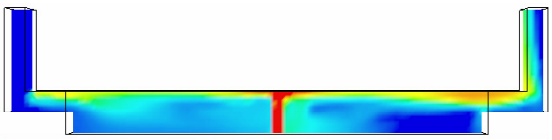

(f) 4min

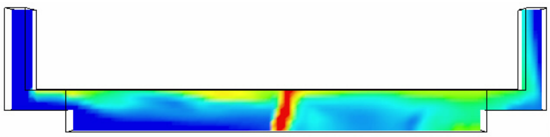

(g) 5min

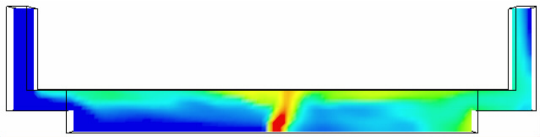

(h) 6min

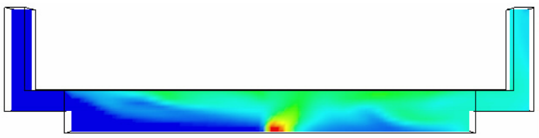

(i) 7min

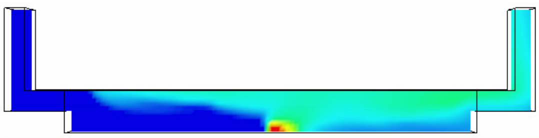

(j) 8min

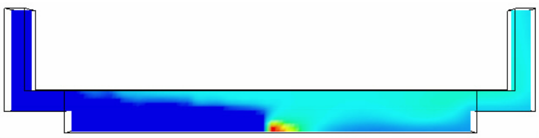

(k) 9min

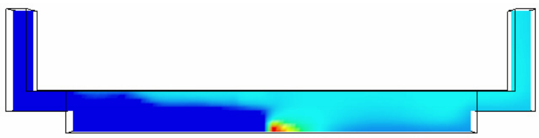

(l) 10min

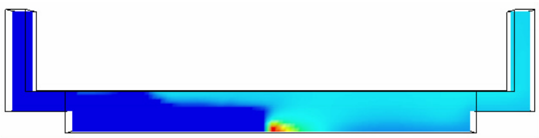

Figure 6

(a) 10sec

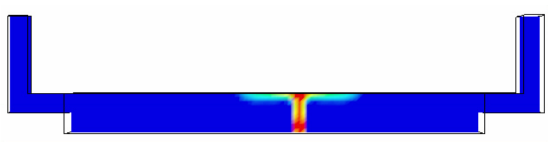

(b) 30sec

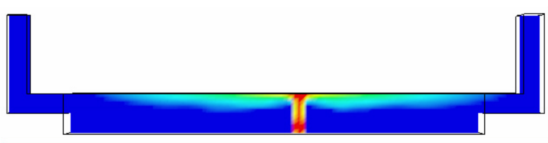

(c) 1min

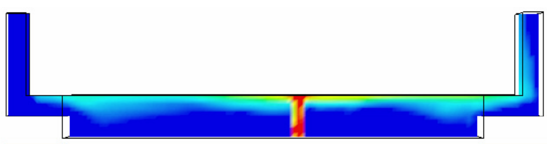

(d) 2min

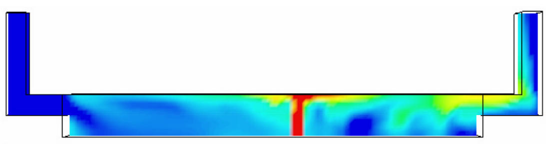

(e) 3min

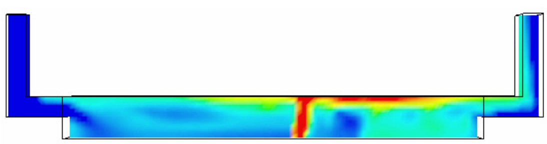

(f) 4min

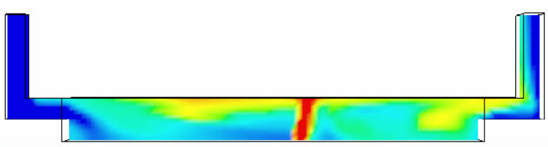

(g) 5min

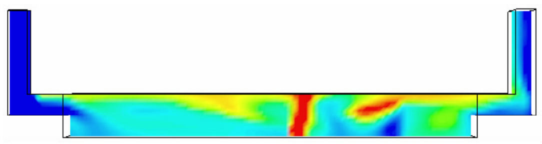

(h) 6min

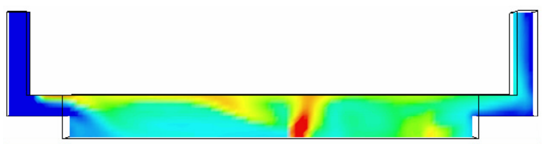

(i) 7min

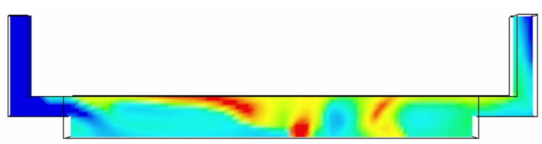

(j) 8min

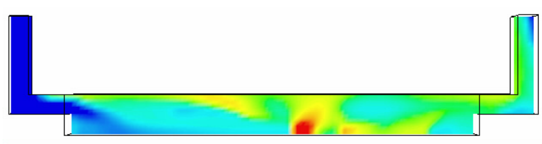

(k) 9min

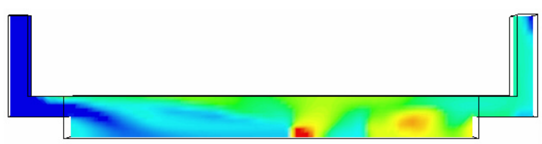

(l) 10min

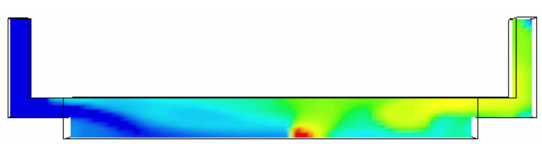

Figure 7

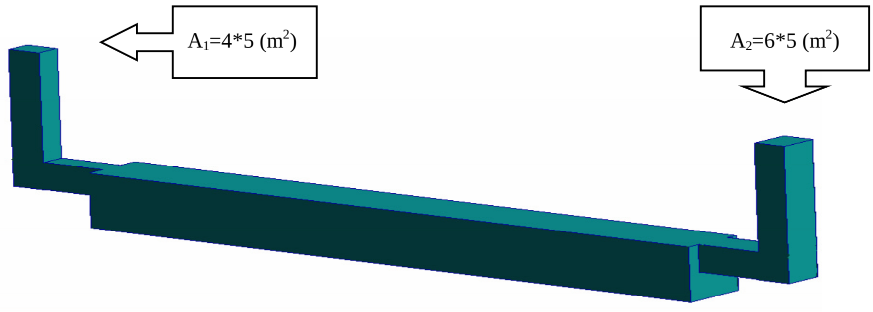

A_1=4*5 (m^2)
A_2=6*5 (m^2)

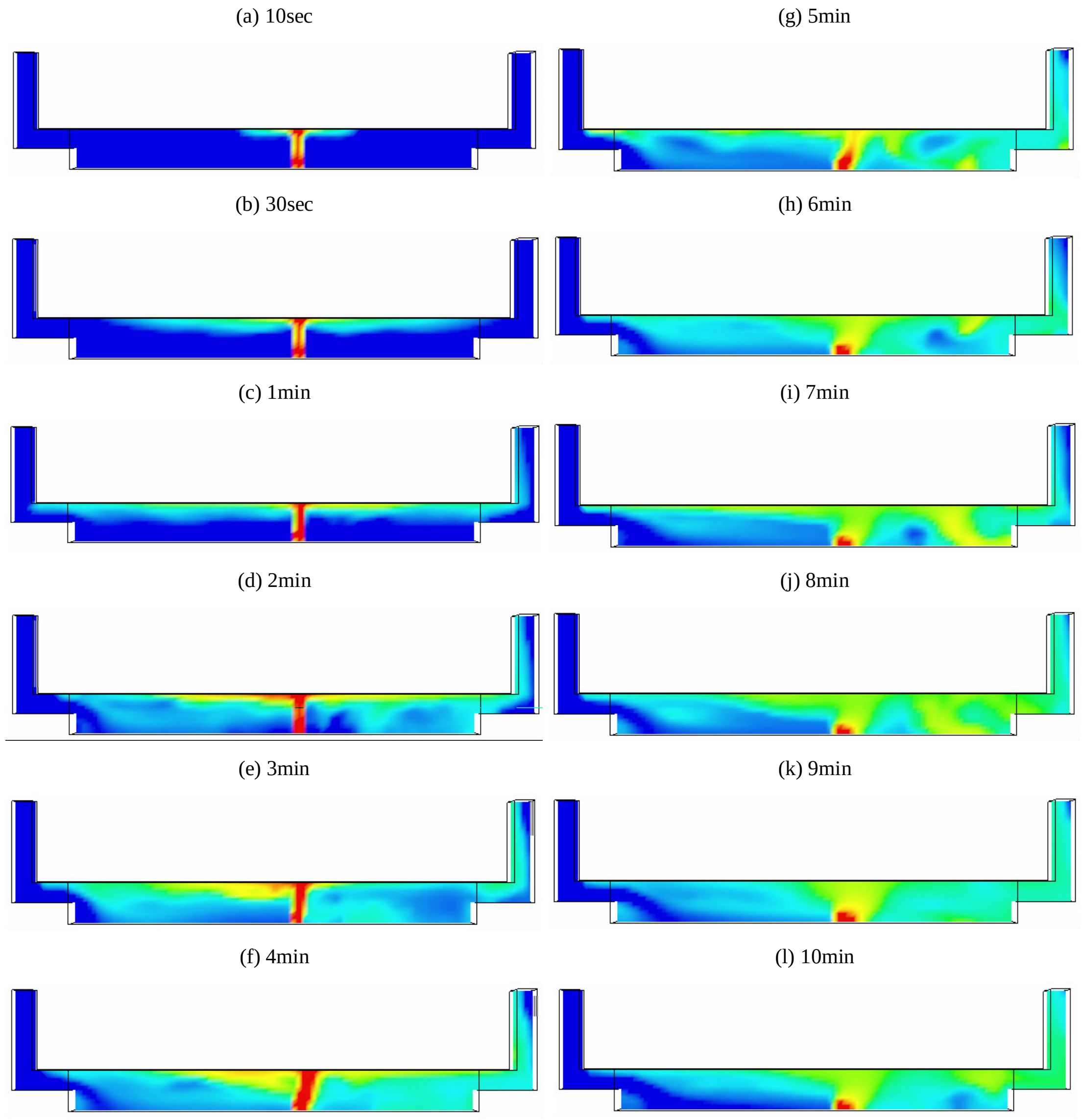

(a) 10sec
(g) 5min
(b) 30sec
(h) 6min
(c) 1min
(i) 7min
(d) 2min
(j) 8min
(e) 3min
(k) 9min
(f) 4min
(l) 10min

Figure 8

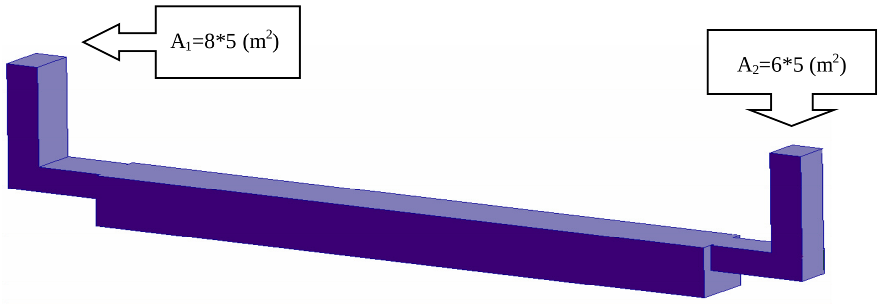
A1=8*5 (m2)
A2=6*5 (m2)

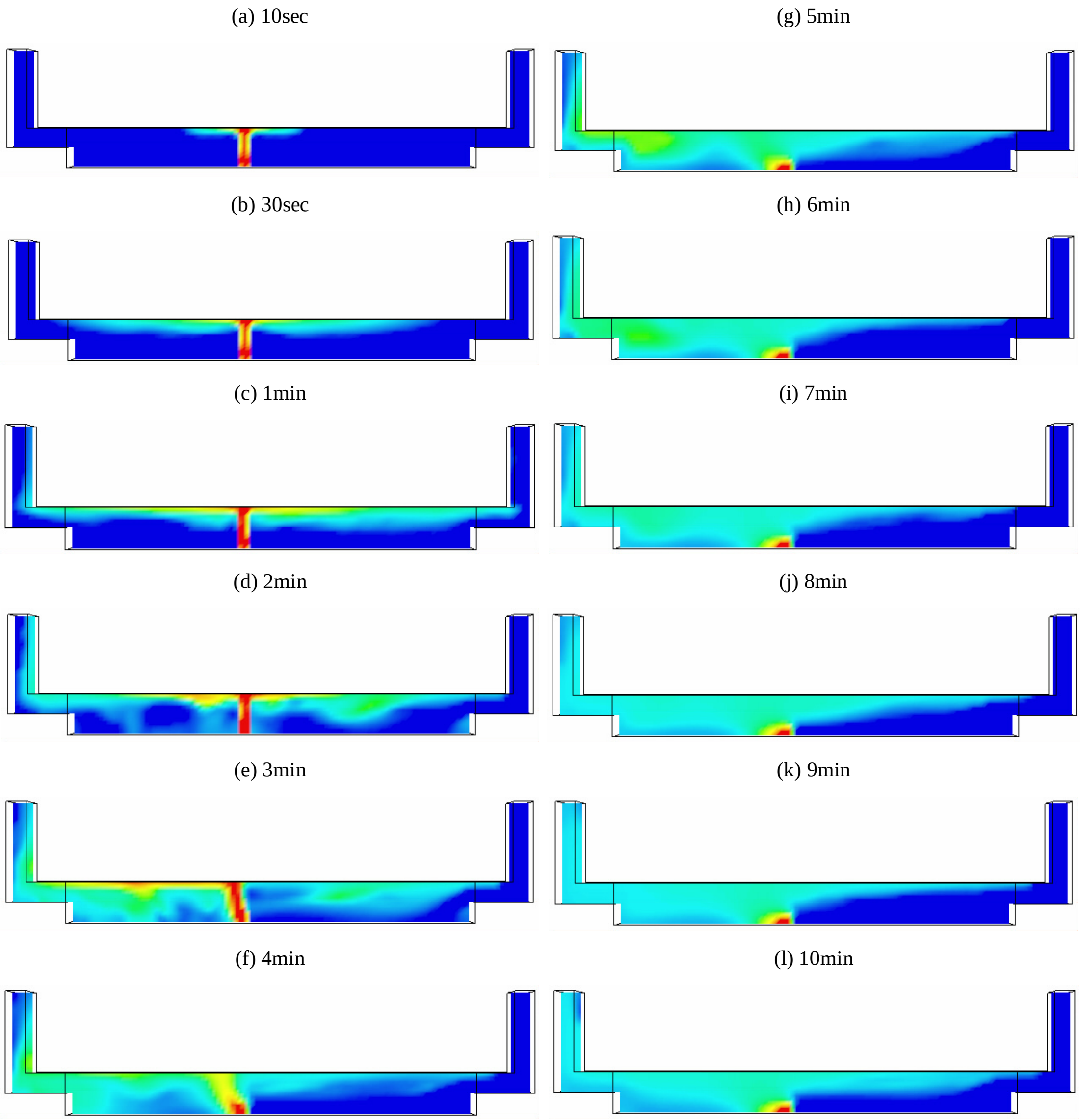
(a) 10sec
(g) 5min
(b) 30sec
(h) 6min
(c) 1min
(i) 7min
(d) 2min
(j) 8min
(e) 3min
(k) 9min
(f) 4min
(l) 10min

Figure 9

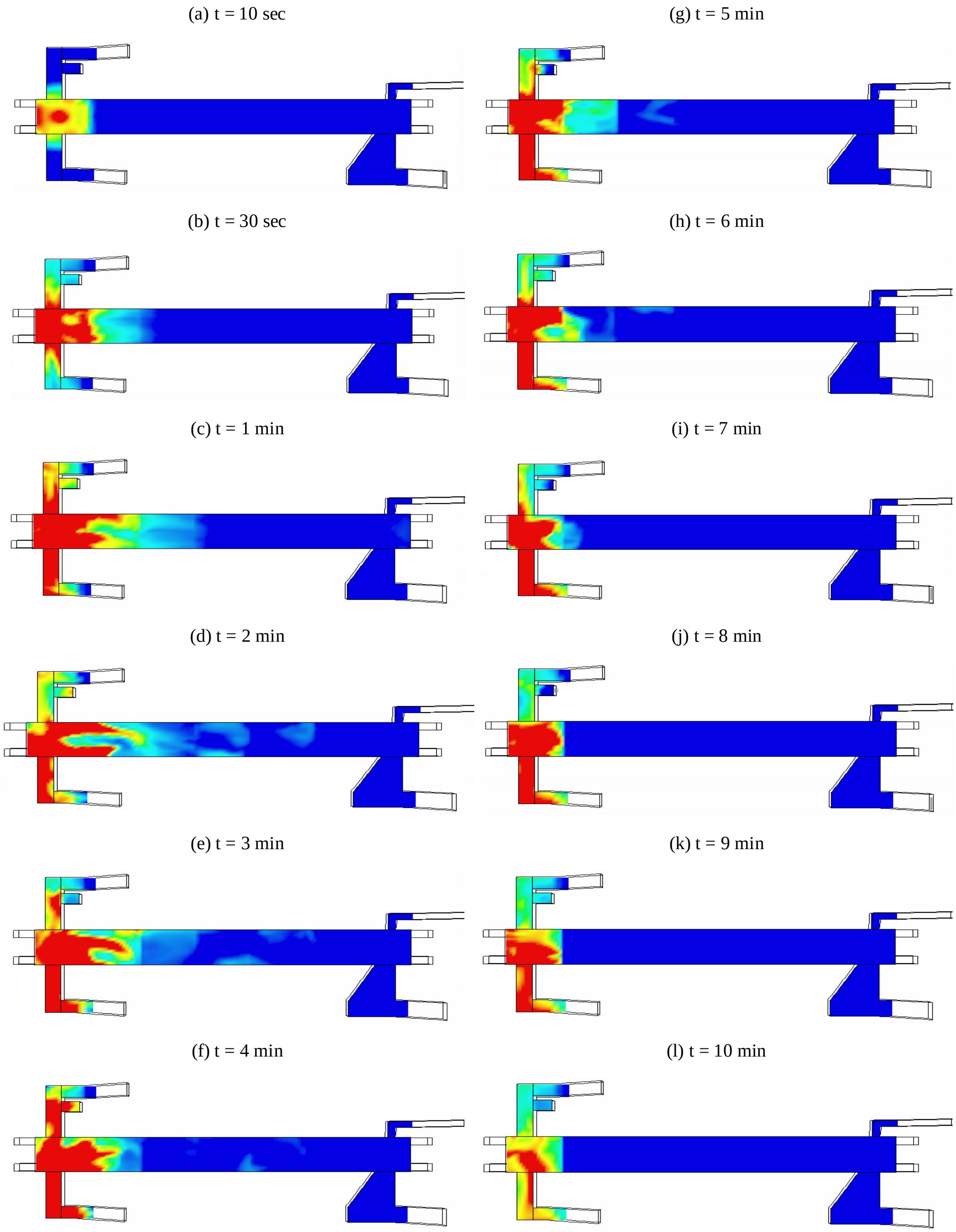
(a) t = 10 sec
(b) t = 30 sec
(c) t = 1 min
(d) t = 2 min
(e) t = 3 min
(f) t = 4 min
(g) t = 5 min
(h) t = 6 min
(i) t = 7 min
(j) t = 8 min
(k) t = 9 min
(l) t = 10 min

Figure 10

(a) t = 4 min

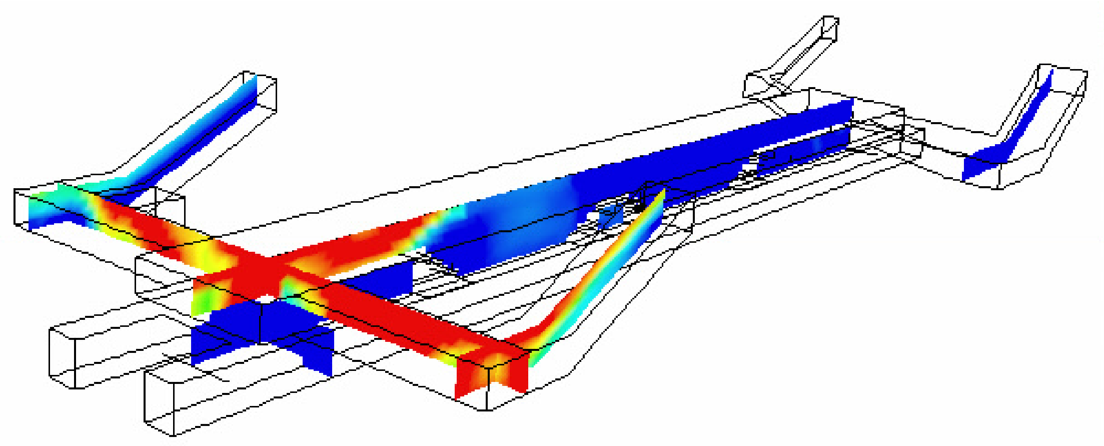

(b) t = 8 min

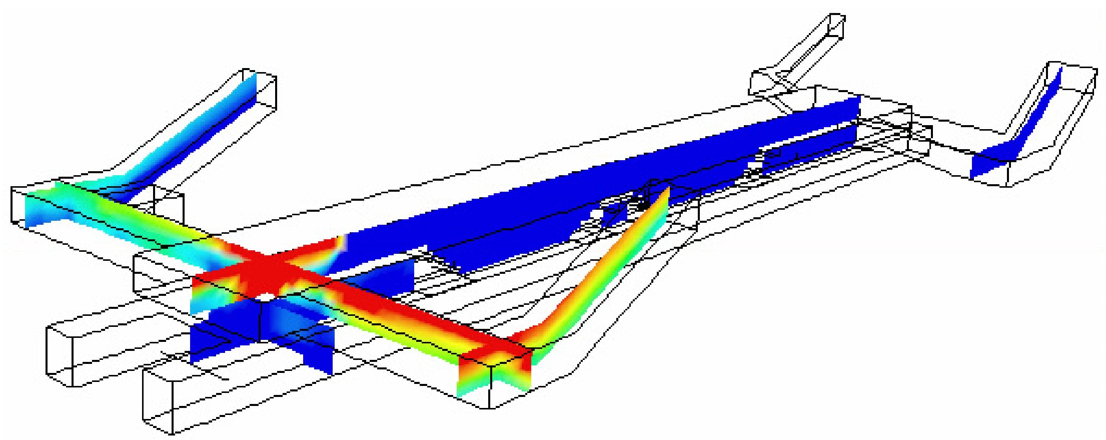

Figure 11

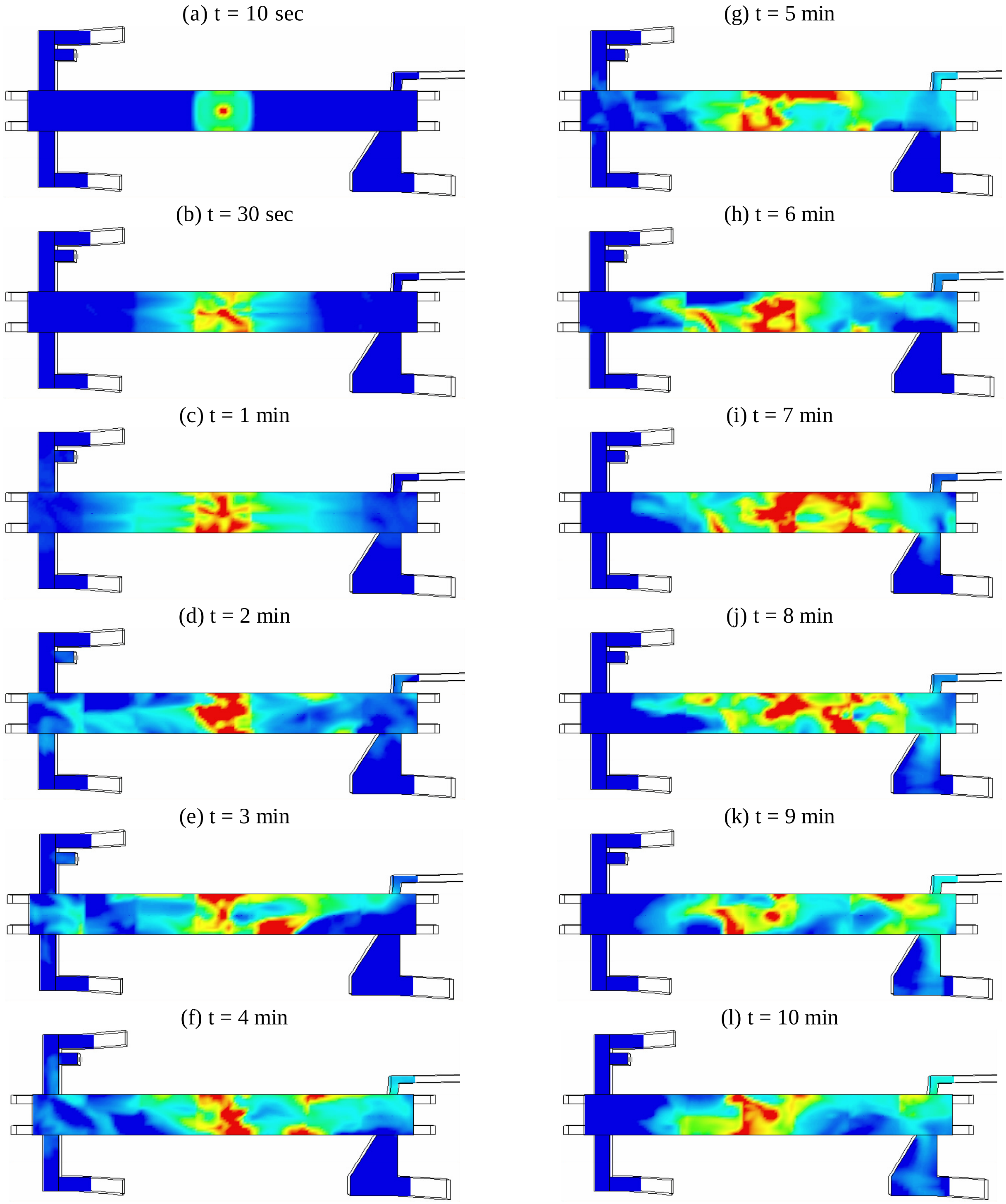
(a) t = 10 sec
(b) t = 30 sec
(c) t = 1 min
(d) t = 2 min
(e) t = 3 min
(f) t = 4 min
(g) t = 5 min
(h) t = 6 min
(i) t = 7 min
(j) t = 8 min
(k) t = 9 min
(l) t = 10 min